

main reason for the deviation in this system is ascribed to the polar nature and the heterogeneity of the adsorbent which results in nonideal interactions among the adsorbate molecules through adsorbent-adsorbate interaction.

#### ACKNOWLEDGMENT

The authors gratefully acknowledge the National Science Foundation and the National Aeronautics and Space Administration for support of this work.

#### NOTATION

$A$  = total surface area of adsorbent, sq. m.  
 $c(i)$  = molecular concentration of species  $i$ , mole/cc.  
 $f(i)$  = fugacity of species  $i$ , lb./sq.in.  
 $G$  = Gibbs free energy, k cal./mole.  
 $H$  = enthalpy, k cal./mole  
 $(i)$  = molecular species  
 $N(i)$  = number of molecules  $i$   
 $N^{GM}(i)$  = summation of  $N^{GM}(i)$  for all  $(i)$   
 $P$  = pressure, lb./sq.in.  
 $Q$  = heat of adsorption, k cal./mole  
 $R$  = gas constant  
 $S$  = entropy, cal./molecule/°C.  
 $T$  = absolute temperature, °K.  
 $v$  = volume expressed at column conditions, cc.  
 $x(i)$  = mole fraction of species  $i$  in the adsorbed phase  
 $y(i)$  = mole fraction of species  $i$  in the gas phase  
 $z$  = compressibility factor  
 $\Delta$  = change on adsorption  
 $\gamma(i)$  = activity coefficient of species  $i$ , k cal./mole  
 $\mu(i)$  = chemical potential of species  $i$ , cal./sq.m.  
 $\pi$  = spreading pressure of the adsorbed phase

#### Superscripts

$o$  = pure component

$A$  = absolute adsorption  
 $G$  = Gibbs adsorption  
 $GM$  = Gibbs adsorption taking into account molecular size  
 $—$  = molar  
 $\infty$  = infinite dilution

#### Subscripts

1 = gas phase  
 2 = adsorbed phase  
 $R$  = experimental retention quantity  
 $d$  = uncompensated dead space in tubings

#### LITERATURE CITED

1. deBoer, J. H., "The Dynamical Character of Adsorption," p.168, Clarendon Press, Oxford (1953).
2. deBoer, J. H., and S. Kruyer, *Trans. Faraday Soc.*, **54**, 540 (1958).
3. Hill, T. L., *J. Chem. Phys.*, **17**, 520 (1949).
4. Hoory, S. E., and J. M. Prausnitz, *Chem. Eng. Sci.*, **22**, 1025 (1967).
5. Hougen, O. A., K. M. Watson, and R. A. Ragatz, "Chemical Process Principles, Part II, second Ed., pp. 863-4, John Wiley, New York (1954).
6. Kiselev, A. V., Y. S. Nikitin, R. S. Petrova, K. D. Shcherbukova, and Y. I. Yashin, *Anal. Chem.*, **36**, 1526 (1964).
7. Masukawa, S., and R. Kobayashi, *J. Gas Chromatog.*, **6**, 257 (1968).
8. ———, *J. Chem. Eng. Data*, **13**, 197 (1968).
9. Myers, A. L., and J. M. Prausnitz, *AIChEJ.*, **11**, 121 (1965).
10. Sturdevant, G. A., Ph.D. dissertation, Rice Univ., Houston, Tex. (1966).
11. Szepeszy, L., and V. Illes, *Acta Chim. Acad. Sci. Hung.*, **35**, 37, 53, 245, 433 (1963).

Manuscript received September 12, 1967; revision received February 16, 1968; paper accepted February 19, 1968.

# Maximum Temperature Rise in Gas-Solid Reactions

DAN LUSS and NEAL R. AMUNDSON

University of Minnesota, Minneapolis, Minnesota

A shell progressive kinetic model is used to determine the temperature rise in a spherical pellet for a gas-solid diffusion controlled reaction. The effects of heat and mass transfer resistances in the gas film as well as inside the pellet are investigated. The predicted temperature rise may be severe enough to cause sintering to catalyst pellets in which reactions such as combustion of coke occur.

During exothermic gas-solid reactions, such as regeneration of catalyst pellets from carbonaceous deposits, the interior temperature of the solid may differ considerably from that of the gas. These temperature effects may cause severe damage to the catalyst and reduce its activity (2). The present work is concerned with the maximum temperature rise in such a system.

For the case of a pseudohomogeneous reaction Damköhler (5) obtained an upper bound on the maximum steady state temperature difference between the interior and exterior temperatures of a catalyst. Prater (8) suggested the use of this bound for catalyst regeneration. Recently, Wei (13) used an elegant method to demonstrate that during the transient period the temperature in certain hot spots can greatly exceed the maximum steady state temperature. His analysis predicts that the smaller the hot spots the higher the upper bound, and he gave an

Dan Luss is with the University of Houston, Houston, Texas.

example for a typical catalyst regeneration process for which Prater's method predicts a maximum temperature rise of 2°C., while his method predicts an upper bound of 34°C. for a hot spot of 2Å and Lewis number of 2. However, the above predicted temperature rise is insufficient to explain the severe damage often caused to catalysts during regeneration.

In this work the shell progressive model is used to compute the maximum temperature rise in gas solid reactions. This mechanism assumes the reaction to occur only in a very narrow moving shell inside the catalyst. It was used successfully to describe various reactions such as combustion and oxidation of ores (3, 4), combustion of coke deposited in catalyst (12), etc. Cannon and Denbigh (4) were the first to treat nonisothermal effects in such reactions. Their work has been extended by Shen and Smith (10). In both these papers the heat capacity of the unreacted core was neglected and this may cause errors in the computed temperature rise, especially during the initial stages of reaction.

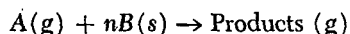
Under certain conditions the diffusion of the gaseous reactant controls the reaction rate. This occurs, for example, in the combustion of coke at temperatures above 500°C. (12). Bondi, et al. (2) studied transient coke burning in catalysts in order to explain their rapid deactivation by approximating the spherical moving boundary problem with the corresponding semi-infinite slab problem. Moreover, they assumed that the mass transfer resistance of the gas film could be neglected, compared to the diffusional resistance in the unreacted core, and this assumption may not be valid during the initial stages of combustion. The present work investigates the maximum temperature rise in a diffusion controlled gas-solid reaction in a spherical pellet using the shell progressive mechanism to describe the reaction rate. Two models, one simple and the other more refined, will be discussed and compared. The analysis accounts for the occurrence of very high temperatures in a catalyst pellet for reactions such as reforming.

## MODEL 1. UNIFORM PARTICLE TEMPERATURE

This model assumes that the temperature inside each particle is uniform. This assumption is appropriate in those cases where the thermal resistance of the particle  $R/\lambda_s$  is very small compared to  $1/h$ , the heat transfer resistance between the gas and the solid; that is,  $hR/\lambda_s < 1$ . The temperature difference,  $T = T_s - T_g$ , between the solid and the gas is determined by

$$\frac{4}{3} \pi a^3 \rho c_s \frac{dT}{dt} + 4\pi a^2 h T = Q \quad (1)$$

where  $Q$  is the heat generated by the reaction



and where the concentrations of  $A$  and  $B$  are denoted by  $C_A$  and  $C_B$ , respectively. The progress of the moving reaction zone with time is

$$\frac{dy}{dt} = \frac{6 D_e n C_A}{C_B a^2} \frac{1}{\left[ y^2 \left( 1 - \frac{1}{N_{Sh*}} \right) - y \right]} \quad (2)$$

where

$$y = r_c/a \quad (3)$$

$$N_{Sh*} = k_c a / D_e$$

Bischoff and Bowen (1, 3) have critically examined the adequacy of Equation (2) and established its validity for gas solid reactions. Thus,

$$Q = -C_B(-\Delta H)_B 4\pi a^3 y^2 \frac{dy}{dt} \quad (4)$$

Substitution of Equation (4) into (1) yields

$$\frac{dT}{dt} + \frac{3h}{a\rho_s c_s} T = \frac{3y^2(-\Delta H)_B C_B}{\rho_s c_s} \frac{dy}{dt} \quad (5)$$

By using Equation (2) to replace  $t$  with  $y$  as the independent variable, Equation (5) can be rewritten in the following dimensionless form

$$\frac{d\theta}{dy} + A \left[ y^2 \left( 1 - \frac{1}{N_{Sh*}} \right) - y \right] \theta = -A y^2 \quad (6)$$

where

$$A = \frac{3h}{a\rho_s c_s} \frac{C_B a^2}{6D_e n C_A} \quad (7)$$

$$\theta = \frac{h a T}{6(-\Delta H)_B D_e n C_A}$$

The boundary condition is

$$\theta = 0, \text{ for } y = 1 \quad (8)$$

This is a linear first-order differential equation, the solution of which is

$$\theta = A \exp A \left[ y^2/2 - \frac{1}{3} \left( 1 - \frac{1}{N_{Sh*}} \right) y^3 \right] \cdot \int_y^1 y^2 \exp A \left[ \frac{1}{3} \left( 1 - \frac{1}{N_{Sh*}} \right) y^3 - y^2/2 \right] dy \quad (9)$$

For the special case  $N_{Sh*} = 1$  Equation (9) may be written

$$\theta = \sqrt{\frac{\pi}{2A}} e^{\frac{Ay^2}{2}} \left[ \operatorname{erf} \sqrt{\frac{A}{2}} - \operatorname{erf} \sqrt{\frac{A}{2}} y \right] + y - \frac{A}{2} (1-y^2) - e \quad (10)$$

For other values of  $N_{Sh*}$  the integral in Equation (9) must be evaluated numerically.

Let us define  $y_m$  as the value of  $y$  for which the maximum temperature difference  $\theta_m$  occurs. It follows from Equation (6) that

$$\theta_m = \frac{y_m}{1 - y_m \left( 1 - \frac{1}{N_{Sh*}} \right)} < N_{Sh*} \quad (11)$$

Note that  $\theta_m$  is a monotonically increasing function of  $y_m$ . Equation (11) yields an upper bound on the maximum temperature difference between the gas and the solid. It can be rewritten as

$$T_m < \frac{6n C_A (-\Delta H)_B k_c}{h} \quad (12)$$

From the analogy between heat and mass transfer to a sphere (9) and assuming that for the gas the Schmidt and Prandtl numbers are equal

$$\frac{k_c a}{D_g} = \frac{h a}{\lambda_g} \quad (13)$$

one obtains

$$T_m = \frac{6D_g n C_A (-\Delta H)_B}{\lambda_g} \frac{\theta_m}{N_{Sh*}} = 6 \frac{D_g \lambda_s}{D_e \lambda_g} \frac{\theta_m}{N_{Sh*}} T_P \quad (14)$$

where

$$T_p = \frac{D_e C_A (-\Delta H)_B}{\lambda_s} n$$

is the upper bound on the temperature difference between the exterior and interior of a catalyst pellet for a pseudo-homogeneous reaction.

It is clear from Equation (14) that the maximum temperature rise predicted by the shell progressive mechanism may greatly exceed this bound predicted for a pseudo-homogeneous reaction. Since it was assumed that the only thermal resistance is that of the gas film, the higher the solid conductivity the more adequate is the present model.

Figure 1 describes the value of  $\theta_m$  computed from Equation (9) as a function of  $A$  and  $N_{Sh*}$ . The dashed line represents the upper bound on  $\theta_m (= N_{Sh*})$  predicted by Equation (11). For large values of  $N_{Sh*}$   $\theta_m$  approaches a constant asymptotic value. In this range the mass transfer resistance of the gas has a negligible effect on the maximum temperature rise. For values of  $N_{Sh*}$  smaller than 100 and  $A$  larger than about 100 the value of  $\theta_m$  is sensitive to changes in the value of  $N_{Sh*}$ . In such cases the assumption  $N_{Sh*} = \infty$  (no mass transfer resistance) may lead to a considerable error in the computed value of  $\theta_m$ .

Figure 2 describes the location of the burning zone for which the maximum temperature difference occurs as a function of  $A$  and  $N_{Sh*}$ . For large values of  $N_{Sh*}$   $y_m$  approaches an asymptotic constant value while for small values of  $N_{Sh*}$   $y_m$  changes slightly with  $N_{Sh*}$  and for large values of  $A$  the value of  $y_m$  is almost one. Thus, the maximum temperature is obtained for the initial stages of combustion.

The value of  $N_{Sh*}$  can be determined from various correlations in the literature for  $N_{Sh} = k_c a / D_g$ . Clearly

$$N_{Sh*} = N_{Sh} \frac{D_g}{D_e} \quad (15)$$

According to Ranz (9) the value of  $N_{Sh}$  for a single sphere should be in the range 1 to 10 for normal operating conditions. However, experimental work on fluidized beds (7) indicates that in such systems the value of  $N_{Sh}$  may be smaller by almost an order of magnitude. The ratio  $D_g/D_e$  is always larger than one, and its value depends on the pore structure of the catalyst. For a typical cracking

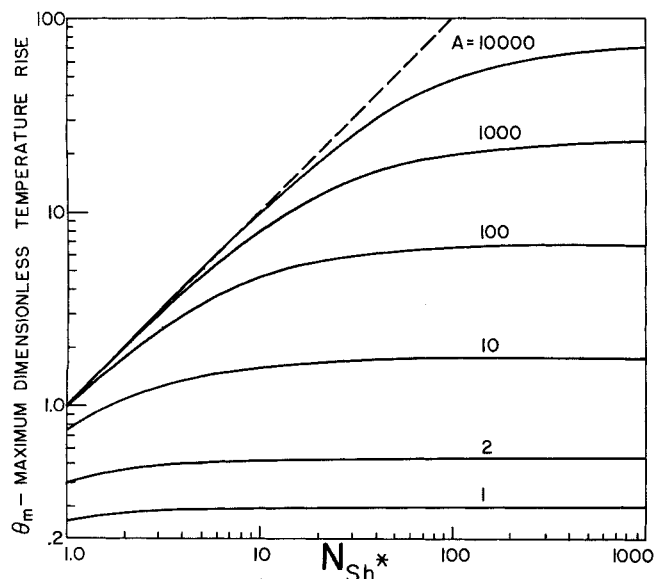


Fig. 1. Maximum temperature difference:  $\theta_m$  as a function of  $A$  and  $N_{Sh*}$ .

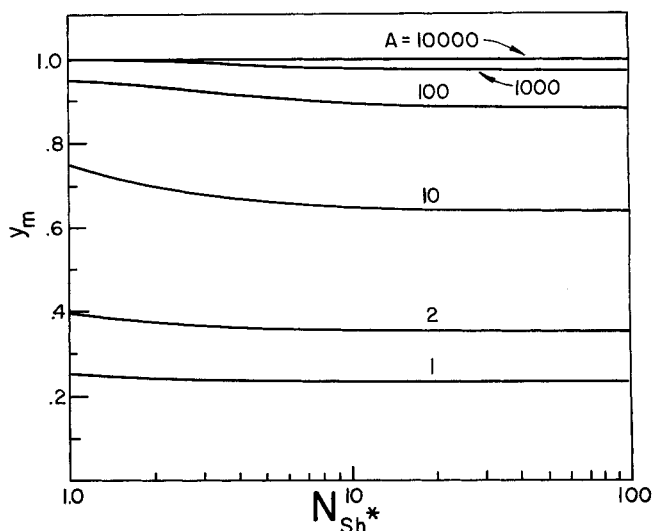


Fig. 2. Location of  $y_m$  as a function of  $A$  and  $N_{Sh*}$ .

catalyst  $D_g/D_e$  is of the order of 10, while for very large pores it is one. Thus the value of  $N_{Sh*}$  should be in the range 1 to 100.

## MODEL 2. NONUNIFORM TEMPERATURE MODEL

This model includes the effect of the thermal resistance of the pellet. It is again assumed that the reaction proceeds by the moving zone mechanism. The instantaneous heat generated by the moving reaction zone  $y$  is

$$Q(y) = -4\pi a^3 \frac{C_B (-\Delta H)_B}{\rho_s c_s} y^2 \frac{dy}{dt} \quad (16)$$

The cooling rate is governed by the boundary condition

$$-k_s \frac{dT}{dr} = hT \quad r = a \quad (17)$$

The temperature at any point  $\xi$  and time  $t$  inside a sphere subject to an instantaneous source  $Q$  at position  $y$  and time  $t = 0$  is (5)

$$T(\xi, y; t) = \frac{Q}{2\pi a^3} \sum_{n=1}^{\infty} f(\beta_n) \frac{\sin(\beta_n y)}{y} \frac{\sin(\beta_n \xi)}{\xi} e^{-\frac{\lambda_s \beta_n^2 t}{\rho_s c_s a^2}} \quad (18)$$

where

$$f(\beta_n) = \frac{(N_{Nu*} - 1)^2 + \beta_n^2}{N_{Nu*} (N_{Nu*} - 1) + \beta_n^2} \quad (19)$$

and  $\beta_n$  are the positive roots of

$$\beta_n \cot \beta_n = 1 - N_{Nu*} \quad (20)$$

According to Duhamel's theorem and Equations (16) to (18) the temperature in the pellet at  $\xi$  when the reaction front reaches  $y$  at time  $t$  is

$$T(\xi, y, t) = -\frac{2(-\Delta H) C_B}{\rho_s c_s} \sum_{n=1}^{\infty} f(\beta_n) \int_s^t y \cdot \sin(\beta_n y) \frac{dy}{d\tau} \frac{\sin(\beta_n \xi)}{\xi} e^{-\frac{\lambda_s \beta_n^2 (t-\tau)}{\rho_s c_s a^2}} d\tau \quad (21)$$

In order to perform the integration one must express  $y$  in terms of  $\tau$  or  $\tau$  in terms of  $y$ . According to the shell pro-

gressive model (1, 12)

$$\frac{1}{2} (1 - y^2) + \frac{1}{3} \left( 1 - \frac{1}{N_{Sh*}} \right) (y^3 - 1) = \frac{6D_e n C_A}{a^2 C_B} t \quad (22)$$

It is more convenient to express  $\tau$  in terms of  $y$ . Thus, Equation (18) can be transformed into

$T(\xi, y)$

$$= \frac{-2(-\Delta H)_B C_B}{\rho_s c_s} \sum_{n=1}^{\infty} f(\beta_n) \frac{\sin(\beta_n \xi)}{\xi} \int_y^1 y^* \sin(\beta_n y^*) \cdot \exp \left\{ \frac{-\beta_n^2 \lambda_s C_B}{6 D_e \rho_s c_s n C_A} \left[ \frac{1}{3} \left( 1 - \frac{1}{N_{Sh*}} \right) \cdot (y^3 - y^{*3}) + \frac{1}{2} (y^{*2} - y^2) \right] \right\} dy^* \quad (23)$$

where  $T(\xi, y)$  is the temperature at  $\xi$  when the reaction front is at  $y$ .

Equation (23) can be rewritten in the dimensionless form

$$\theta(\xi, y) = \frac{2}{3} A \sum_{n=1}^{\infty} f(\beta_n) \frac{\sin(\beta_n \xi)}{\xi} \int_y^1 y^* \sin(\beta_n y^*) \cdot \exp \left\{ -\frac{A \beta_n^2}{3 N_{Nu*}} \cdot \left[ \frac{1}{3} \left( 1 - \frac{1}{N_{Sh*}} \right) (y^3 - y^{*3}) + \frac{1}{2} (y^{*2} - y^2) \right] \right\} dy^* \quad (24)$$

A typical temperature profile of the pellet as a function of the location of the reaction zone is shown in Figure 3. During the initial stages of the reaction the temperature attains a maximum value at some point near the surface. This maximum temperature increases with time. Eventually, due to increasing heat losses from the pellet and retardation of the reaction rate by the increased diffusional resistance, the maximum temperature starts to decrease with increasing values of  $y$ . In the example shown in Figure 3 the maximum temperature was obtained for  $y = 0.88$ .

In the unreacted core for  $y > 0$

$$\rho_s c_s \frac{\partial T}{\partial t} = k_s \frac{1}{r^2} \frac{\partial}{\partial r} \left( r^2 \frac{\partial T}{\partial r} \right) \quad (25)$$

and since initially the temperature of the center is a local minimum, according to Equation (25),  $\partial T / \partial t|_{\xi=0} > 0$ ,

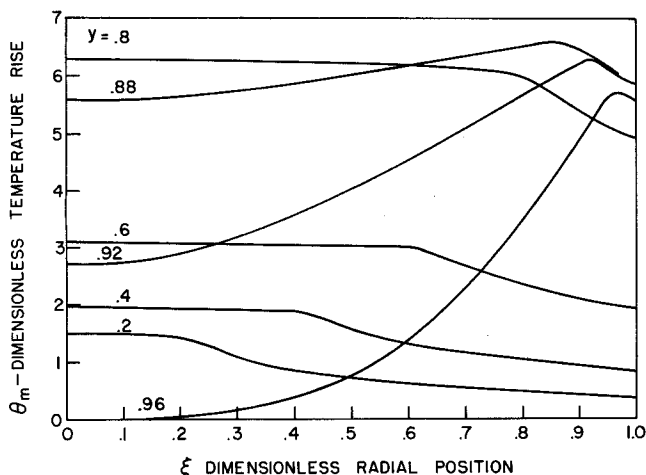


Fig. 3. Transient temperature profile,  $A = 100$ ,  $N_{Sh*} = 100$ ,  $N_{Nu*} = 1.0$ .

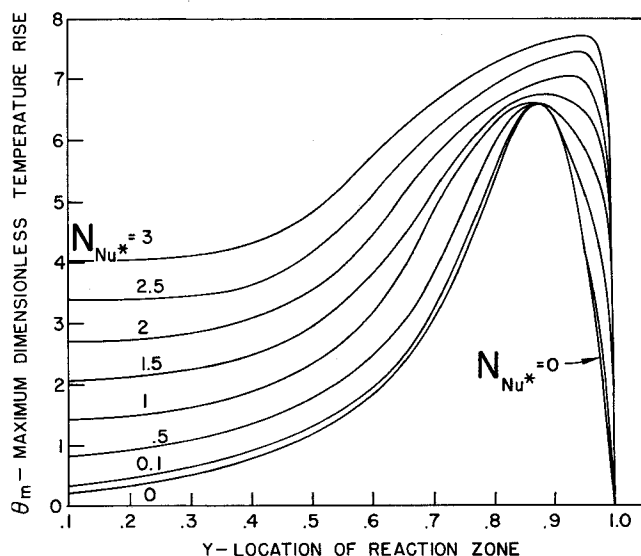


Fig. 4. Effect of  $N_{Nu*}$  on the maximum temperature rise  $\theta_m$ ,  $A = 100$ ,  $N_{Sh*} = 100$ .

that is, the temperature increases with time. After the maximum temperature of the pellet starts to decrease with time, the temperature of the center becomes a local maximum and decreases with time.

The temperature differences in the solid are of the same order as the temperature difference between the gas and the solid surface. The ratio between these two temperature differences depends mainly on the value of  $N_{Nu*}$ , the ratio between the heat transfer resistance of the solid to that between the gas and the solid surface. The maximum value of  $N_{Nu*}$  under practical conditions is of order one. The smaller the value of  $N_{Nu*}$ , the more uniform is the temperature of the pellet.

Figure 4 describes the variation of the maximum temperature  $\theta_m$  in the pellet as a function of  $y$  and  $N_{Nu*}$ .  $\theta_m$  increases with  $N_{Nu*}$ . An increase of  $N_{Nu*}$  increases somewhat the value of  $\max(\theta_m)$  and causes it to occur for larger values of  $y$ , i.e. the maximum temperature is obtained for a shorter period after the start of the reaction. In all the cases shown in Figure 4 the simple model for which  $N_{Nu*} = 0$ , gave a good estimate of the value of  $\max(\theta_m)$ . For  $N_{Nu*} \leq 0.1$  the simple model gave a very good estimate for the value of  $\theta_m$  for all stages of the reaction. For  $N_{Nu*} \geq 1$  the simple model fails to give a good estimate on the value of  $\theta_m$  for small values of  $y$ .

Figure 5 describes the average temperature  $\bar{\theta}$  of the pellet for various values of  $N_{Nu*}$  and  $y$ . The simple model ( $N_{Nu*} = 0$ ) gives a good estimate on the value of  $\bar{\theta}$  for all values of  $y$  and  $N_{Nu*}$ . For large values of  $y$ ,  $\bar{\theta}_m$  occurs for some point near the surface, and the surface temperature increases with increasing values of  $N_{Nu*}$ . The heat losses from the particle are a linear function of the surface temperature. Thus, the larger  $N_{Nu*}$  is, the greater are the heat losses and the smaller is  $\bar{\theta}$ . For small values of  $y$ ,  $\theta_m$  is obtained near the center of the catalyst and the surface temperature decreases with increasing values of  $N_{Nu*}$ . Thus the larger  $N_{Nu*}$ , the smaller are the heat losses, and the larger is the value of  $\bar{\theta}$ .

Figure 6 describes the effect of  $N_{Sh*}$  on the value of  $\theta_m$  for various values of  $y$  for two values of  $N_{Nu*}$ . It is seen that for the initial stages of the reaction, that is large values of  $y$ , the value of  $N_{Sh*}$  greatly affects the value of  $\theta_m$ . However, for small values of  $y$ , the value of  $\theta_m$  becomes independent of the value of  $N_{Sh*}$ , and depends only on the value of  $N_{Nu*}$ , the reason being that the relative importance of the gas-film resistance to mass transfer de-

creases with the increase of the diffusional resistance inside the pellet.

### EXAMPLE

For the combustion of coke in a typical cracking catalyst compute by use of the two models

1. The maximum possible temperature rise
2. The maximum temperature rise when 99% of the coke has been burned.

We assume the following data

$$D_e = 5 \times 10^{-3} \text{ sq.cm./sec.} \quad (11)$$

$$D_g = 2 \times 10^{-1} \text{ sq.cm./sec.} \quad (11)$$

$$C_A = 3 \times 10^{-6} \text{ mole/cc.} \quad (11)$$

$$C_B = 4.5 \times 10^{-3} \text{ mole/cc.} \quad (10)$$

$$\lambda_s = 8 \times 10^{-4} \text{ cal./ (cm.} \times \text{ } ^\circ\text{C.} \times \text{ sec.)} \quad (10)$$

$$\lambda_g = 8 \times 10^{-5} \text{ cal./ (cm.} \times \text{ } ^\circ\text{C.} \times \text{ sec.)} \quad (10)$$

$$\rho_s = 1.0 \text{ g./cc.} \quad (10)$$

$$c_s = 0.3 \text{ cal./ (g.} \times \text{ } ^\circ\text{C.)} \quad (10)$$

$$n = 1.0 \quad (10)$$

$$-\Delta H_B = 83,000 \text{ cal./g.mole} \quad (7)$$

$$N_{Nu} = N_{Sh} = 2.5$$

Thus,

$$ha = N_{Nu} \lambda_g = 2 \times 10^{-4} \text{ cal./ (sq.cm.} \times \text{ } ^\circ\text{C.} \times \text{ sec.)}$$

$$N_{Nu*} = N_{Nu} \lambda_g / \lambda_s = 0.25$$

$$N_{Sh*} = N_{Sh} D_g / D_e = 100$$

1. Substitution of the data into Equation (7) yields  $A = 100$ . Thus, for the simple model according to Figure 1,  $\theta_m = 6.6$ . By use of Equation (14)  $T_p = 1.56^\circ\text{C.}$  and  $T_m = 158 \times T_p = 247^\circ\text{C.}$

To compute the maximum temperature rise by the second model, one must use Figure 4. It is clear from that figure that for the above case both models predict the same maximum temperature rise of  $247^\circ\text{C.}$

2. When 99% of the coke has been burned  $y = 0.215$ . By use of Figure 4 it was found that for this value of  $y$ ,  $\theta_m = 0.35$  for the simple model and 0.65 for model 2. By use of Equation (14) it was found that these values correspond to a maximum temperature rise of 13 and  $24^\circ\text{C.}$ , respectively.

### CONCLUSIONS

It was shown that very high temperatures may occur during diffusion controlled gas-solid reactions which are described by the shell progressive mechanism. This tem-

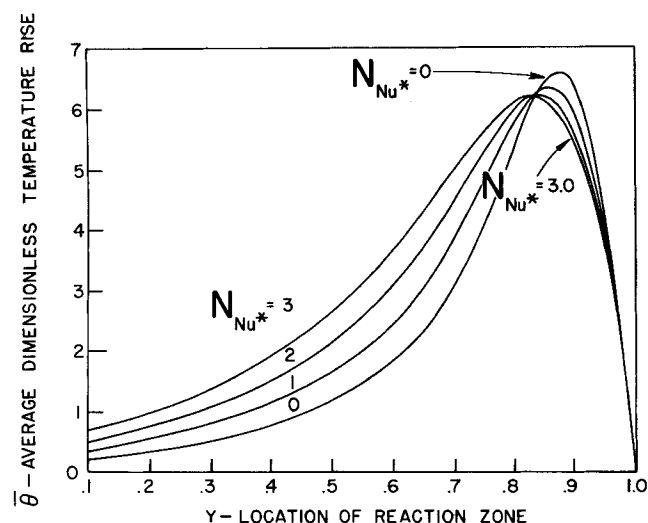


Fig. 5. Effect of  $N_{Nu*}$  on the average temperature of the pellet,  $A = 100$ ,  $N_{Sh*} = 100$ .

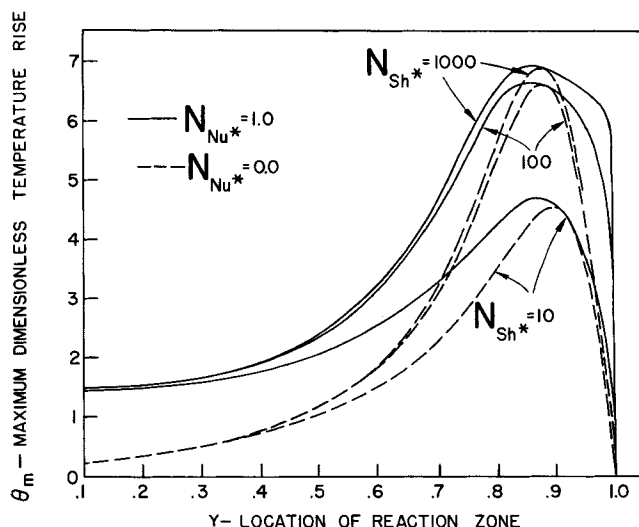


Fig. 6. Effect of  $N_{Sh*}$  on the maximum temperature rise  $\theta_m$ ,  $A = 100$ .

perature rise is usually much higher than that predicted by assuming the reaction to be pseudo-homogeneous. A simple model was derived from which a good estimate can be obtained for the magnitude of the maximum temperature rise  $\theta_m$ . This value was found to be rather sensitive to the gas-film mass transfer coefficient. It was shown that under practical operating conditions the temperature difference between the gas and the solid surface is at least of the same order as the temperature difference in the solid. The temperature rise may cause severe damage to catalyst particles.

### ACKNOWLEDGMENT

This work was supported by the National Science Foundation.

### NOTATION

$A$	= quantity defined by Equation (7)
$a$	= pellet radius
$C$	= concentration
$c$	= specific heat
$D_e$	= effective diffusivity
$D_g$	= diffusivity of gas
$\Delta H_B$	= heat of reaction of solid reactant
$h$	= heat transfer coefficient
$k_c$	= mass transfer coefficient
$n$	= stoichiometric ratio of solid consumed/mole gas
$N_{Nu}$	= $ha/\lambda_g$
$N_{Nu*}$	= $ha/\lambda_s$
$Q$	= heat produced by reaction
$r_c$	= radial position of reacting front
$N_{Sh}$	= $k_ca/D_g$
$N_{Sh*}$	= $k_ca/D_e$
$T$	= temperature of the solid minus the ambient gas temperature
$t$	= time
$T_p$	= $D_e C_A (-\Delta H)_B n / \lambda_s$
$y_m$	= $y$ for which $\theta_m$ is obtained

### Greek Letters

$\theta$	= dimensionless temperature, defined by Equation (7)
$\theta_m$	= maximum value of $\theta$
$\bar{\theta}$	= average value of $\theta$
$\lambda$	= thermal conductivity
$\xi$	= $r/a$
$\rho$	= density

## Subscripts

$g$  = gas phase  
 $s$  = solid phase

## LITERATURE CITED

1. Bischoff, K. B., *Chem. Eng. Sci.*, **18**, 711 (1963); **20**, 783 (1965).
2. Bondi, A., R. S. Miller, and W. G. Schlaffer, *Ind. Eng. Chem. Process Design Develop.*, **1**, 196 (1962).
3. Bowen, J. R., *Chem. Eng. Sci.*, **20**, 712 (1965).
4. Cannon, K. G., and K. G. Denbigh, *ibid.*, **6**, 145, 155 (1957).
5. Carslaw, H. C., Jaeger, T. C., "Conduction of Heat in Solids," 2nd Ed., Oxford Univ. Press, New York (1959).
6. Damköhler, G., *Z. Phys. Chem.*, **A193**, 16 (1943).
7. Frantz, J. F., *Chem. Eng. Prog.*, **57**, 35 (1961).
8. Prater, C. D., *Chem. Eng. Sci.*, **8**, 284 (1958).
9. Ranz, W. E., and W. R. Marshall, Jr., *Chem. Eng. Progr.*, **48**, 141, (1952).
10. Shen, J., and J. M. Smith, *Ind. Eng. Chem. Fundamentals*, **4**, 293 (1965).
11. Sehr, R. A., *Chem. Eng. Sci.*, **9**, 145 (1958).
12. Weisz, P. B., and R. D. Goodwin, *J. Catalysis*, **2**, 397 (1963).
13. Wei, J., *Chem. Eng. Sci.*, **21**, 1171 (1966).

Manuscript received November 22, 1967; revision received February 5, 1968; paper accepted February 7, 1968.

# Use of Electrochemical Techniques to Study Mass Transfer Rates and Local Skin Friction to a Sphere in a Dumped Bed

KENNETH R. JOLLS and THOMAS J. HANRATTY

University of Illinois, Urbana, Illinois

Electrochemical techniques are developed to study the details of the flow around a single particle in a packed bed. Initial work has been done with a dumped bed of 1 in. spheres. Results are presented on the variation of the mass transfer coefficient and the shear stress around the surface of one of the spheres, the overall mass transfer rates to a sphere in a bed of inert spheres, and the effect of Reynolds number on the local mass transfer coefficient and the shear stress.

Present knowledge of the behavior of packed beds is limited because most of the measurements on these systems reflect average happenings over a large number of particles. A considerable amount is known about the flow field around isolated particles, and therefore it has been possible to explain measurements of heat and mass transfer and of drag on them. Similar knowledge is needed about flow around a particle in the presence of other particles in a packed bed.

In recent years a number of contributions have been made to our understanding of this problem. Kramers and Thoenes (10) suggested that the mass transfer coefficient for a single particle in a bed of inert particles is a better measure of what actually occurs between the particle surface and the fluid. They obtained overall mass transfer rates for fluids flowing around single spheres which were part of a regular arrangement of similar, but inactive spheres. Glaser (4) measured the overall heat transfer rate between air and an electrically heated sphere located

in a dumped bed of unheated spheres. Denton (2) and Wadsworth (21) have measured local heat transfer coefficients for air flow with a specially instrumented test sphere located in a regular packing arrangement. Korchak (9) has made turbulence measurements in the interstices of a regular array of spheres. Denton, who carried out his experiments at Reynolds numbers of 5,000, 20,000, and 50,000, located his test sphere at the center of a body-centered cubically packed bed. Wadsworth worked at Reynolds numbers of 8,000 to 60,000 and used the rhombohedral No. 6 blocked-passage array described by Martin, McCabe, and Monrad (11). Rhodes and Peebles (16) studied local mass transfer rates from single benzoic acid test spheres in cubic and rhombohedral arrays for Reynolds numbers of 488 to 3,410 by measuring the local diminution in radius of the test sphere after exposure to a measured rate of water flow for a given length of time.

This paper shows how electrochemical techniques that have been used to study turbulence close to a wall may be applied to the study of the flow around a sphere in a packed bed of spheres. They offer the possibility that in a single experiment one is able to (a) measure the shear

Kenneth R. Jolls is with Brooklyn Polytechnic Institute.